Appl. Phys. A 72, 133–142 (2001) / Digital Object Identifier (DOI) 10.1007/s003390100788

Applied Physics A
Materials
Science & Processing

Hydrogen storage using carbon adsorbents: past, present and future

A.C. Dillon, M.J. Heben*

National Renewable Energy Laboratory, Golden, Colorado 80401, USA

Received: 16 October 2000/Accepted: 15 November 2000/Published online: 9 February 2001 –

Abstract. Interest in hydrogen as a fuel has grown dramatically since 1990, and many advances in hydrogen production and utilization technologies have been made. However, hydrogen storage technologies must be significantly advanced if a hydrogen based energy system, particularly in the transportation sector, is to be established. Hydrogen can be made available on-board vehicles in containers of compressed or liquefied H_2, in metal hydrides, via chemical storage or by gas-on-solid adsorption. Although each method possesses desirable characteristics, no approach satisfies all of the efficiency, size, weight, cost and safety requirements for transportation or utility use. Gas-on-solid adsorption is an inherently safe and potentially high energy density hydrogen storage method that could be extremely energy efficient. Consequently, the hydrogen storage properties of high surface area "activated" carbons have been extensively studied. However, activated carbons are ineffective in storing hydrogen because only a small fraction of the pores in the typically wide pore-size distribution are small enough to interact strongly with hydrogen molecules at room temperatures and moderate pressures. Recently, many new carbon nanostructured absorbents have been produced including graphite nanofibers and carbon multi-wall and single-wall nanotubes. The following review provides a brief history of the hydrogen adsorption studies on activated carbons and comments on the recent experimental and theoretical investigations of the hydrogen adsorption properties of the new nanostructured carbon materials.

PACS: 81.07.De; 81.05.Uw; 68.43.h

The decreasing fossil fuel supply and the growing number of densely populated metropolitan cities with poor local air quality have spurred an initiative to develop an alternative fuel. Hydrogen, which may be produced from renewable sources while burning pollution-free, has emerged as one of the most promising candidates for the replacement of the current carbon-based energy services. Although hydrogen could easily supply all of the world's vehicular energy demands [1], a major impediment to the development of this new technology is the lack of a convenient, cost-effective on-board storage system.

Possible current approaches to vehicular hydrogen storage include (i) physical storage via compression or liquefaction, (ii) chemical storage in irreversible hydrogen carriers (e.g. methanol, ammonia), (iii) reversible metal and chemical hydrides and (iv) gas-on-solid adsorption. Although each storage method possesses desirable attributes, no approach satisfies all of the efficiency, size, weight, cost and safety requirements for personal transportation vehicles. The United States Department of Energy (DOE) has set target system energy densities at values of 6.5 wt % and 62-kg H_2/m^3. Presently, a compact, lightweight hydrogen-storage system for transportation is not available. Hydrogen storage is therefore the key enabling technology that must be significantly advanced in terms of performance and cost effectiveness if hydrogen is to become an important part of the world's energy economy.

Recently, lightweight carbon adsorbent materials have become interesting for possible use in a hydrogen-storage system. Early work in this area in the 1960s, 1970s and 1980s focused on the H_2-adsorption properties of various 'activated' carbon materials which were prepared from mineralogical or organic precursors. These materials were typically obtained by thermochemical processing and contained many different types of carbon structures that provided a variety of environments for binding hydrogen. Unfortunately, the vast majority of the sites for adsorption could not stabilize hydrogen above cryogenic temperatures. Recent advances in the science of carbon nanostructures have allowed new types of adsorbents to be 'engineered'. Numerous studies on molecular hydrogen adsorption on graphite nanofibers (GNFs) and carbon multi-wall and single-wall nanotubes (MWNTs and SWNTs) have been reported. This review provides a brief history of the hydrogen-adsorption studies on activated carbons and also outlines the recent experimental and theoretical investigations on engineered nanostructured materials. Finally, we highlight some specific research areas that require further investigation, with particular attention to the case of carbon single-wall nanotubes.

*Corresponding author.

1 Past: a brief history of hydrogen storage on activated carbon materials

One of the first investigations of the adsorption of hydrogen on high-surface-area carbon was reported in an excellent paper by Kidnay and Hiza in 1967 [2]. The work was focused on the behavior of adsorbents from a cryogenic engineering perspective. Adsorption isotherms for hydrogen on coconut-shell charcoal were reported at 76 K and pressures up to 90 atm. Already in this early work the authors discussed a major source of confusion associated with reporting and understanding adsorption of hydrogen on carbon that is still relevant today. Specifically, there are at least three different ways that the amount of gas adsorbed on a material can be reported. The first way specifies the thermodynamically important quantity known as the 'excess amount' which is 'the excess material present in the pores over that which would be present under the normal density at the equilibrium pressure' [3, 4]. This rigorous method of reporting is made possible by correcting the raw data for gas compressed into the non-adsorbing free volume of the container. With this approach, a plot of the excess amount versus pressure often exhibits a maximum. Beyond the maximum the bulk gas density increases more quickly with increasing pressure than does the adsorbed density, and higher hydrogen-storage densities can be achieved in a given container by removing the carbon adsorbent [4]. A second definition terms the 'total amount' the 'amount contained in the pore volume' (i.e., all matter under the influence of the adsorption forces). Adsorption isotherms reported in this manner are calculated by adding to the excess amount an additional amount that accounts for gas compressed into the active volume of the sample. The latter volume is determined from the saturation values obtained in N_2-adsorption isotherms. This particular definition is somewhat artificial and not of particular value to either the scientist who is interested in the intrinsic behavior of an adsorbent, or the engineer wishing to build a storage tank. A third method of reporting simply involves plotting the amount of hydrogen contained in the adsorbent-filled container as a function of the pressure. Since no attempt is made to correct for the non-adsorbing volume of the container, the role played by the adsorbent is unclear, and the data is a convolution of the storage capacity of both the free volume of the container and the adsorbent. Although the work of Kidnay and Hiza was not focused on the storage of hydrogen, a maximum excess amount of hydrogen of 20.2-g H_2/kg carbon was reported at 25 atm and 76 K, corresponding to a gravimetric storage density of ~ 2.0 wt % [2].

Carpetis and Peschka [5, 6] were among the first to suggest that hydrogen could be inexpensively stored on activated carbon materials by adsorption at cryogenic temperatures. It was initially asserted that hydrogen could be stored on carbon at volumetric densities approaching values available with liquid hydrogen [6]. Adsorption isotherms were reported for a variety of different types of high-surface-area carbon materials at 78 and 65 K at pressures up to 41.5 atm [5]. Unfortunately, the total mass of the adsorbent used in each experiment was not reported so it is impossible to determine from the paper if the cryogenically cooled container could have stored more hydrogen if the carbons were not present. The adsorbed hydrogen was maximized at ~ 5.2 wt % for a 'F12/350' carbon material exposed to 41.5 atm of hydrogen at 65 K. The more open, porous carbon materials that were investigated tended to adsorb more hydrogen than the denser carbons that were studied. A detailed analysis [5] concluded that cryo-adsorption on activated carbon at 42 atm and 65 K was more economically attractive for bulk hydrogen storage than either FeTi alloys, ambient-temperature pressure vessels at 11 atm, or liquefied hydrogen. A cryo-adsorption storage system was determined to have $\sim 1/4$ the volumetric energy density of a liquid-hydrogen-storage system [5].

The research group of J.A. Schwarz at Syracuse University was quite active in studying the storage of hydrogen on activated carbon in the late 1980s and early 1990s. These efforts were focused on developing a detailed understanding of the fundamental aspects of hydrogen adsorption on activated carbon materials so the operating temperature of the adsorbent could be increased. Towards this goal the effects of surface acidity [7] and metal modification were investigated [8]. The group also performed detailed thermodynamic analyses to determine important parameters such as the isosteric heat of adsorption [9]. Despite these efforts, the best activated carbon identified adsorbed ~ 4.8-wt % H_2 at a temperature of 87 K and a pressure of 59 atm [10]. Under the same conditions, a carbon-fiber-wrapped pressure vessel containing this activated carbon stored an additional 4.3 wt % (carbon basis) as compressed gas in the voids within the container. Taking into account the weight of the pressure vessel and vacuum jacket, the total system stored H_2 at 4.2 wt % and 16.8 kg/m^3. As with previous investigations, this storage system did not significantly benefit from the incorporation of carbon under the chosen operating conditions. A simple calculation using the parameters specified by Schwarz [10] reveals that hydrogen could be stored in the tank at 4.8 wt % and 16.5 kg/m^3 at the same pressure and temperature without the carbon.

It is important to note that the inclusion of activated carbon material in a storage tank can enhance the overall hydrogen energy storage density under certain pressure and temperature conditions. Chahine and Bénard have formalized this concept by defining a 'gain' parameter for adsorption storage which offers a comparison of the densities of the adsorbed gas and the compressed gas as a function of pressure and temperature [11]. Similar experimental data has been obtained by Hynek et al. [4]. The gain is maximized at low temperatures and pressures for a given activated carbon. This corresponds to the situation where the adsorbent surface is populated but the density in the gas phase above the adsorbent is not appreciable. Although the overall storage capacity of a tank is maximized at the high-pressure and low-temperature conditions employed by Carpetis and Peschka and Schwarz, the effectiveness of the adsorbent is minimized under these conditions. The magnitude of the maximum gain is controlled by the surface area and microporous volume. Ideally, one would like to have highly microporous material with relatively high material density (i.e., low in macroporous volume).

In a recent comprehensive study, Hynek et al. tested a variety of carbon sorbents such as activated carbon, carbon black, carbon aerogels and carbon molecular sieves in order to determine whether they augmented the capacities of compressed hydrogen gas storage systems [12]. The various carbon sorbents were tested at ambient temperature (300 K), acetone and dry-ice temperature (190 K) and at liquid-nitrogen temperature (80 K). They concluded that at pressures typical of vehicular compressed hydrogen-storage

systems ($\sim$ 200 bar), only one of ten carbon sorbents tested did in fact augment the capacity of the storage vessel. This improvement was marginal at 190 K and 300 K and non-existent at 80 K [12]. In general, there have been very few reports of an activated carbon type adsorbent capable of improving the storage capacities of a high-pressure tank at 300 K [4, 13]. In an even more recent report Orimo et al. [14] attempted to fabricate a novel carbon sorbent by mechanically ball milling graphite under a hydrogen atmosphere. X-ray diffraction of the resulting nanocrystalline graphite indicated an expansion of the graphite inter-layer spacing with long-range order disappearing for increasing milling time. The hydrogen concentration was reported to reach up to 7.4 wt % after milling for 80 h. Neutron-diffraction measurements indicated that both molecular hydrogen and covalently bonded hydrogen were present [14]. Although both gravimetric and volumetric storage systems appear quite good for this system, the reversibility of charging and discharging seems unlikely.

2 Present

2.1 Hydrogen storage in carbon nanofibers

It is difficult to obtain high-surface-area 'activated' carbon adsorbents with small pore sizes and narrow pore-size distributions. Porous carbons synthesized by conventional thermal processing generally exhibit more than 50% of total pore volume as macroporosity [15] with pore dimensions greater than $\sim$ 40 Å. Macropores only participate in monolayer hydrogen adsorption, similar to hydrogen bound on a plane, and therefore are not useful for ambient-temperature hydrogen storage. These synthetic limitations explain the relatively poor hydrogen uptakes observed thus far for conventional carbon adsorbents and have spurred the development of carbon materials which are more specifically designed for hydrogen adsorption.

Graphite nanofibers are an example of an engineered material that has recently been investigated for hydrogen-storage applications. These materials are produced by decomposition of mixtures of ethylene, hydrogen and carbon monoxide on selected metal and alloy catalysts [16]. Three distinct structures may be produced: 'tubular' (90°), 'platelet' ($\sim$ 0°) and 'herringbone' (45°) where the angle in parentheses indicates the direction of the nanofiber axis relative to the vector normal to the graphene sheets. The spacing between graphite layers in each case is the same value found in conventional graphitic carbon, $\sim$ 3.4 Å. The nanofibers typically range in diameter from 5 to 500 nm [16]. Very high hydrogen-storage densities exceeding 50 and 60 wt % have been reported for the platelet and herringbone forms respectively, while the tubular structure exhibited storage densities exceeding 10 wt % [17]. The hydrogen uptake was recorded as a drop in pressure from an initial value of 112 atm over a period of $\sim$ 24 h at a temperature of 298 K. Figure 1 schematically shows a commensurate phase for hydrogen adsorbed on graphite with a nearest-neighbor spacing of 4.26 Å as observed by neutron diffraction for low coverages of H_2 adsorbed on graphite [18]. This corresponds to a coverage of one H_2 per 15.6 Å^2. At higher pressure the monolayer becomes more dense and an incommensurate close-packed structure with a nearest-neighbor distance of 3.51 Å or one H_2 per 11.0 Å^2 is observed (also Fig. 1). Considering to the results of Chambers et al. [17], for sake of argument let us assume that the number of layers of H_2 between planes of graphite could somehow be as large as five. Consequently, a storage density of 60-wt % H_2 would require a nearest-neighbor distance within one of these five monolayers of only 0.98 Å or one H_2 per 0.82 Å^2. This dense coverage is also depicted in Fig. 1. However, since the kinetic diameter of H_2 is 2.9 Å, the illustration can not de-

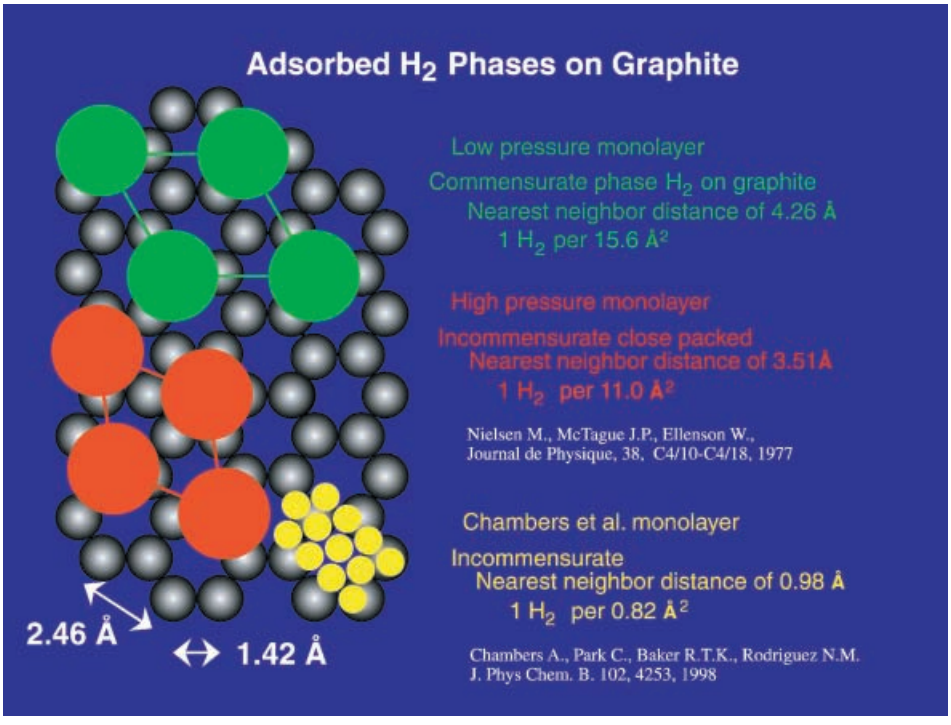

Fig. 1. Several proposed configurations for hydrogen adsorbed on graphite including a commensurate phase with a nearest-neighbor spacing of 4.26 Å for low coverages of hydrogen; a denser and an incommensurate close-packed structure with a nearest-neighbor distance of 3.51 Å at higher pressure; and the monolayer that would be required to achieve the densities reported in [17] if 5 layers were present between every two sheets of graphite.

scribe a true physical system, and it would be required to have 4–5 of these layers to reach the reported high values.

Ahn et al. attempted to corroborate these extraordinary results [19]. Hydrogen-adsorption studies were conducted on similarly fabricated fibers for temperatures between 77 and 300 K. H_2 gas was admitted into an evacuated chamber to achieve a typical pressure of 4.5 or 80 atm for the 77-K runs or 180 atm for the 300-K runs. The absolute level of hydrogen desorption measured for the GNFs was typically less than 0.01 H/C or ~ 0.08 wt % [19]. In another attempt to confirm the previously published large adsorption numbers a maximum value of 1.52 wt % was obtained for GNFs at ambient temperature and ~ 125 atm [20]. In defense of the initial investigations, the original group reported that the presence of water vapor had a very deleterious effect on the GNFs and that the high hydrogen-adsorption capacities were made possible by an expansion of the fiber's graphitic layers [21]. Unfortunately an in-situ probe of such a *c*-axis expansion was not available. X-ray data of a pristine sample and the same sample following both an adsorption and a desorption step showed an expansion of the lattice of only 0.007 nm, which is considerably less than the value of 0.03 nm observed for H_2 adsorbed in potassium-intercalated graphite [24]. In a recent study, Fan et al. reported hydrogen-storage capacities of $10-13$ wt % on vapor-grown carbon fibers which were not graphitic. Based on the initial studies of GNFs, the group projects that higher storage values will be obtained upon graphitization [22].

2.2 Hydrogen storage in multi-wall carbon nanotubes

Multi-wall carbon nanotubes consist of layers of nested concentric cylinders of graphite with a hollow center. The spacing between each cylinder is similar to the inter-planar spacing in graphite, and the number of shells varies from 2 up to about 50. MWNTs have inner and outer diameters that are typically 2–10 and 15–30 nm, respectively, and are generally microns in length. Large bundles of MWNTs with diameters up to 200 μm [23] and very long individual tubes, over 2 mm [25], have been observed. Multi-walled nanotubes were discovered while vaporizing carbon in an electric arc [26] and were subsequently produced at much higher yield with a variation in the same technique [27]. A simplified method for the arc-generation of MWNTs has been reported quite recently [28]. Multi-walled nanotubes have also been produced via benzene pyrolysis [29] and the decomposition of acetylene [31, 32] with metal catalysts. The crystallinity and stability of the tube caps may be compromised when MWNTs are produced by the catalytic decomposition of hydrocarbons. Carbon nanotubes produced by the catalytic decomposition of acetylene over a cobalt-incorporated zeolite were purified with a hydrofluoric acid treatment to remove the catalyst support followed by a permanganate or air oxidation to remove amorphous carbon impurities [32]. Arc-generated MWNTs have been purified with air-oxidation but in order to remove all of the nanocrystalline graphite particles that are present as impurities, it is necessary to oxidize 99% of the total material [33]. When permanganate oxidation was applied to arc-generated MWNTs the nanocrystalline graphite again could not be removed [32]. Figure 2a displays a transmission electron microscope (TEM) image of highly graphitic MWNTs formed by the method of arc discharge. For comparison a TEM image of a poorly graphitized MWNT formed from the thermal decomposition of propylene over a porous alumina membrane template [34] is shown in Fig. 2b.

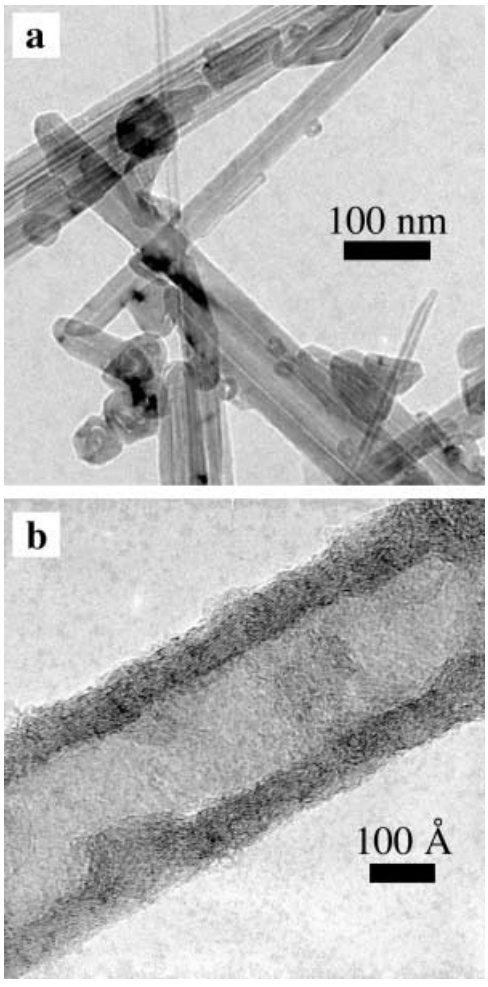

Fig. 2a,b. Transmission electron microscope (TEM) images of **a** highly graphitic MWNTs formed by the method of arc discharge and **b** a poorly graphitized MWNT formed from the thermal decomposition of propylene over a porous alumina membrane template

Chen et al. reported remarkable hydrogen-storage capacities for alkali-metal-doped MWNTs formed by the catalytic decomposition of CH_4 [35]. The walls of the nanotubes formed via this process are conical in shape and for this reason these nanotubes have been sometimes classified as graphitic nanofibers [36]. Li and K were incorporated in the carbon nanotubes through solid-state reactions with the metal carbonates or nitrates. Hydrogen desorption and adsorption was measured by thermogravimetric analysis (TGA) and temperature-programmed desorption (TPD). The H_2 uptake was shown to be 20 wt % for Li-doped nanotubes at 653 K and 14 wt % for K-doped nanotubes at room temperature. The K-doped nanotubes were reported to combust upon exposure to air. The hydrogen adsorption was believed to proceed by a dissociative mechanism, and an infrared spectrum of the hydrogen-charged Li-doped material was interpreted to indicate the presence of both Li−H and C−H species [35]. In a subsequent TGA study, Li-doped MWNTs formed under identical conditions were shown to exhibit a weight increase

of 12 wt % when exposed to 'wet H_2' and only 2.5 wt % in the presence of 'dry H_2' [37]. An infrared spectrum of LiOH:H_2O which was strikingly similar to the spectrum acquired by Chen et al. was also provided. When K-doped nanotubes were exposed to 'dry H_2' a weight increase of only 1.8% was observed [37]. In yet another report on the hydrogen-storage properties of Li-doped MWNTs, large cycling mass changes similar to those observed by Chen et al. were again attributed to the presence of water impurities in the TGA atmosphere. No evidence of hydrogen adsorption by the Li-doped MWNTs was detected [38].

A very recent report probed the hydrogen-adsorption properties of multi-wall nanotubes synthesized by the catalytic decomposition of CO and CH_4 on powdered La_2O_3 catalysts [39]. The CO-generated tubes consisted of concentric cylinders while the CH_4-produced tubes contained graphite layers that were tilted with respect to the tube axis, forming cones. In both cases the catalyst was removed by stirring in dilute nitric acid. The purified nanotubes were then annealed to 1100 °C in vacuum in order to increase crystallinity. TGA analysis in flowing hydrogen revealed that the CO-generated tubes were capable of adsorbing a small quantity of hydrogen (0.25 wt %) when the sample was cooled between 200 °C and room temperature [39]. Another recent study indicated that MWNTs may also be charged with hydrogen by electrochemical methods [40]. Materials employed for this study were synthesized in an arc process and contained $10-40$% MWNTs with diameters which varied from 2 to 15 nm. Stable electrodes were be formed by pressing the MWNT material with palladium powder in a 1 : 4 ratio. The equilibrium curve of the MWNT/palladium electrode indicated two separate electrochemical reactions, one of which was not observed for pure palladium electrodes. Although the overall capacity for the palladium/MWNT electrode was less than that anticipated for pure palladium, the study indicated that electrochemical hydrogen storage in MWNTs may be possible [40].

2.3 Carbon single-wall nanotubes

For conventional physisorption, the gas-adsorption performance of a porous solid is maximized when the pores are not larger than a few molecular diameters [41]. Under these conditions the potential fields from the walls of the so-called micropores overlap to produce a stronger interaction than would be possible for adsorption on a semi-infinite plane. If the escaping tendency of the gas is much less than the adsorption potential, the entire micropore may be filled with a condensed adsorbate phase. For the case of hydrogen, with a kinetic diameter of ~ 2.9 Å, pores would have to be significantly smaller than 40 Å to begin to condense hydrogen by a nanocapillary filling mechanism. The ideal hydrogen adsorbent should have (i) uniform and small micropores in as high a density as possible, (ii) minimal macroporosity and (iii) high thermal conductivity. The first characteristic is required for an enhanced heat of adsorption which might provide for ambient-temperature adsorption, while the first two characteristics together insure that the internal volume of the adsorbent is not wasted. The third characteristic provides for managing heat fluxes that will hopefully be relatively large by virtue of an enhanced heat of adsorption. One conceptual model, which provides all of these features, is an array of bundled carbon single-wall nanotubes. An individual SWNT is essentially a sheet of graphite which is wrapped to meet itself forming a single elongated and seamless tube. The individual tubes self-assemble during synthesis via van der Waals interactions to form bundles which contain hundreds of SWNTs. Figure 3 displays a TEM image of a bundled array of SWNTs. The image shows a cross-sectional view of a large nanotube bundle so that the hexagonal packing of the tubes may be observed. A cartoon of a hexagonal array of SWNTs is also provided.

Single-wall carbon nanotubes were first synthesized by the co-evaporation of a cobalt catalyst and graphite in an electric arc [42, 43]. Fibers typically consisted of 7–14 bundled SWNTs 10–15 Å in diameter. Figure 4a displays a TEM image of arc-generated SWNT material. The image reveals cobalt nanoparticles, 5–50 nm in diameter, embedded in a matrix of amorphous carbon and nanocrystalline graphite. Bundles of carbon-coated SWNTs span the image. It is readily apparent that these initial materials were highly impure. Motivated by the theoretical calculations which suggested that carbon single-wall nanotubes should be able to stabilize HF molecules by a process akin to nanocapillarity [44], Dillon et al. investigated the hydrogen-adsorption properties of the early SWNT materials. Although their materials contained only $\sim 0.1-0.2$-wt % SWNTs, hydrogen adsorption on the carbon nanotube fraction was estimated for ambient conditions to be between $\sim 5-10$ wt %, and a heat of adsorp-

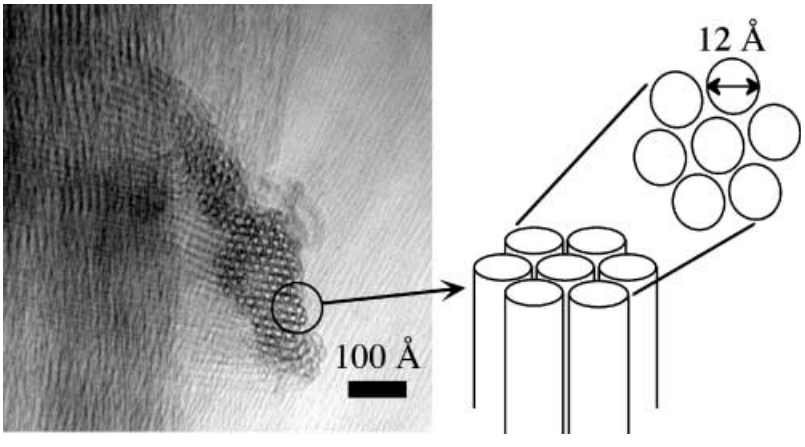

Fig. 3. TEM image of a bundled array of SWNTs displaying a cross-sectional view of a large nanotube bundle making the hexagonal packing of the tubes apparent. The image is accompanied by a blown-up drawing of a hexagonal array of SWNTs

tion of 19.6 kJ/mol was measured [45]. This demonstrated an enhanced interaction between hydrogen and SWNTs relative to planar graphite, where the heat of adsorption is only ~ 4 kJ/mol [46].

Single-wall carbon nanotubes were later produced at much higher yield by the method of laser vaporization [47]. Crystalline ropes microns in length containing hundreds of individual SWNTs were easily obtained [48]. The laser-generated soots also contained metal nanoparticle catalysts and various carbon components, but SWNTs were routinely generated at $\sim 20-50$ wt %. Figure 4b displays a typical TEM image of raw laser-generated SWNT soots. Research was then focused on the further purification of the much higher quality materials. Multiple different purification techniques ranging in complexity and final SWNT yield were quickly established [49–54]. Figure 4c displays a TEM image of purified SWNTs obtained by refluxing laser-produced material in 3 M HNO_3 for 16 h followed by oxidation in air for 30 min at 550 °C. When care is taken to stay in a vaporization regime during synthesis [55] so that micron-sized graphite particles are not generated, this method of purification results in SWNTs which are greater than 98-wt % pure [54]. Figure 4d displays a high-magnification image of the purified SWNTs following a brief anneal to 1500 °C in vacuum in order to re-establish the order in the bundles which was lost during the acid reflux.

Ye et al. were the first to report hydrogen-adsorption investigations on purified [53] laser-generated [48] SWNTs [56]. Here the purification technique involved field-flow filtration and several acid washing and annealing steps [53]. Prior to the adsorption studies the tubes were sonicated for 10 h in dimethyl formamide in order to cut the SWNTs and disrupt the rope structure. Hydrogen adsorption on the purified crystalline ropes of SWNTs was 8 wt % at ~ 40 atm and 80 K. However in contrast to the earlier studies [45], high adsorption capacities on the laser-generated tubes were not observed at 300 K and pressures below 1 atm. At pressures higher than about 40 atm at 80 K, a phase transition was observed and attributed to a separation of the individual SWNTs. Hydrogen was believed to be physisorbed on the exposed surfaces of the tubes [56]. The quantum rotation of hydrogen adsorbed on laser-generated SWNTs was also observed via inelastic neutron scattering, demonstrating that H_2 was physisorbed at 25 K under 11-MPa hydrogen [57].

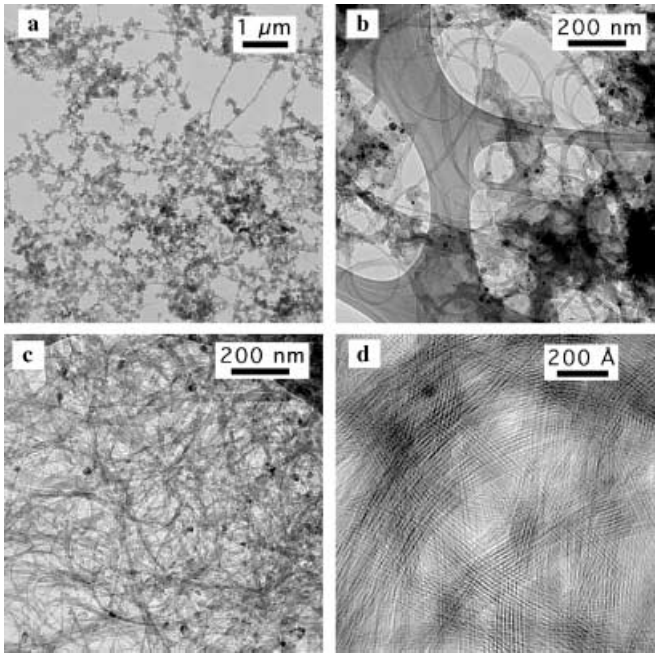

Fig. 4a–d. TEM images of **a** a initial highly impure arc-generated SWNT material, **b** a typical raw soot of laser-generated SWNTs which contains $\sim$ 25-wt % nanotubes, **c** 98-wt % SWNTs obtained by refluxing laser-produced material in 3 M HNO_3 for 16 h followed by oxidation in air for 30 min at 550 °C and **d** the purified SWNTs at high magnification following a brief anneal to 1500 °C in vacuum in order to re-establish order in the bundles that was lost during the acid reflux

High hydrogen-storage capacities on a total sample weight basis were subsequently demonstrated on SWNTs with a large mean diameter of about 1.85 nm produced at high yield by a semi-continuous arc-discharge method [58]. The purity of the nanotube soots was estimated to be $\sim 50-60\%$. A sample which was first soaked in HCl and then heat-treated in vacuum was shown to adsorb 4.2-wt % H_2 at room temperature and 10 MPa. Approximately 80% of the adsorbed hydrogen could also be released at room temperature [58]. It is interesting to note that high-capacity room-temperature adsorption was first demonstrated for arc-generated SWNTs and not laser-produced nanotubes. This may be attributed to a much smaller number of ends or defects in the laser-produced tubes and/or an enhancement in their stability towards opening procedures or cutting. A newly developed high-power ultrasonic cutting procedure which incorporates a $TiAl_{0.1}V_{0.04}$ alloy has been applied to purified, laser-generated SWNT materials allowing high-capacity hydrogen adsorption at ambient conditions [59, 60]. The maximum adsorption capacity is ~ 7 wt % and the hydrogen adsorption occurs in two separate sites. Approximately 2.5 wt % of the hydrogen is evolved at 300 K while the remainder desorbs between 475–850 K. In addition to cutting, the procedure also introduces an alloy of composition $TiAl_{0.1}V_{0.04}$ due to decomposition of the ultrasonic probe. The presence of the alloy might in fact stimulate hydrogen adsorption and desorption. Several control experiments have shown that the observed uptake is not solely due to the presence of the alloy, and there are some experimental indications of partial electron transfer being responsible for the stability of the hydrogen [59, 60].

Electrochemical hydrogen storage has also been demonstrated for carbon single-wall nanotubes. Arc-generated SWNT soot containing a few percent of 0.7–1.2-nm diameter SWNTs was mixed with either copper or gold as a compacting powder in a 1 : 4 ratio to form electrodes. The kinetics of the SWNT electrode were relatively poor. However the capacity at low discharge currents was as high as 110 mA h/g which corresponds to ~ 0.39 wt % [40]. Assuming that all of the stored hydrogen is contained in the small SWNT fraction of the sample, these results indicate that electrochemical hydrogen storage on highly pure SWNTs should be investigated. In a more recent study, SWNT composite electrodes were fabricated by mixing with conducting Ni powders and an organic polytetrafluroethylene (PTFE) in a ratio of 40 : 50 : 10, SWNT : Ni : PTFE. Charge/discharge capacities of 160 mA h/g were demonstrated [61]. Unfortunately, no information on the synthesis or purity of the SWNT material was provided.

2.4 Theoretical reports on H_2 adsorption in graphitic slit pores and nanotubes

When Dillon et al. published the experimental value of 5 – 10 wt % for hydrogen adsorption on SWNTs, they also performed a simple calculation which indicated that filling the inside of 20-Å diameter tubes would come close to meeting the DOE target system energy densities [45]. It was assumed that such an array of SWNTs would have a surface area close to the theoretical maximum for graphite ($\sim 2620\,m^2/g$) and a density of ~ 1 g/cc. An H_2–H_2 nearest-neighbor distance of 3.51 Å was obtained from neutron-diffraction studies of H_2 adsorbed on graphite with a coverage of ~ 1 monolayer [18]. Then assuming the closest approach of H_2 to the inner tube wall to be ~ 2.95 Å [46], filling a 20-Å diameter tube with hydrogen molecules produced a gravimetric and volumetric energy density of 5.1 wt % and $54\,kg\,H_2/m^3$. Dresselhaus et al. later used similar logic to show that two layers of H_2 adsorbed on a flat sp^2 carbon surface result in an adsorption density of 4.1 wt % [62]. Figure 5 shows how the storage densities (predicted in the above fashion) for several types of SWNTs with different diameters compare to experimentally reported values for single-walled carbon nanotubes and with the DOE goals. The large degree of scatter in the reported data may be due to differences in material quality and experimental approach, and highlights the need for more work.

Following the initial experimental investigation and simple calculation regarding hydrogen adsorption on SWNTs, a large number of rigorous theoretical investigations were reported which employed classical or quantum molecular simulations [63–71] and density functional theory [72, 73]. Among the earliest predictions, Stan and Cole performed an analysis of hydrogen adsorption in nanotubes at the low-coverage limit using a phenomenological interaction potential [63]. They determined that the adsorption potential for hydrogen within carbon nanotubes is indeed enhanced but only to $\sim 50\%$ of what was initially observed experimentally [45]. Another early study by Darkrim et al. [64] employed Monte Carlo numerical simulations to determine that single-wall nanotubes would increase by $\sim 15\%$ the amount of hydrogen stored in a given volume over that stored by an activated carbon material, AX-21 (at 298 K and 10 MPa).

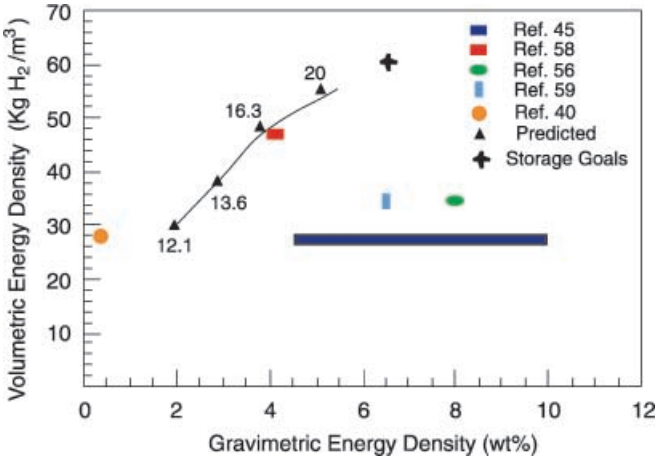

Fig. 5. Storage densities for several types of SWNTs with different diameters as predicted by the method described in the text compared to experimentally reported values for single-walled carbon nanotubes and with the DOE goals. The volumetric values shown for the experimentally reported gravimetric data are based on calculated values assuming the ideal case of closely packed SWNTs having the average diameter reported in the reference. Impurities in the experimental materials are not taken into account, and most materials have a distribution of diameters. Also note that the calculation only considers filling the interior of the SWNTs. If the interstitial sites are also filled the storage densities would need to be adjusted. The lines connecting the predicted values are a guide to the eye

Wang and Johnson employed computer simulations to compare the adsorption of hydrogen gas in single-walled nanotubes with idealized carbon slit pores [66]. Although the adsorption potential was enhanced for SWNTs relative to slit pores of the same size, the calculation predicted that the storage capacity for an array of nanotubes was less than that of slit pores at both 77 and 298 K. Adsorption isotherms were in reasonably good agreement with experimental data for activated carbon, but did not account for high-storage capacities in carbon nanotubes. A second theoretical study also considered hydrogen adsorption in idealized slit pores versus carbon nanotubes [68]. At room temperature a slit pore consisting of two graphite platelets separated by a distance equal to the diameter of two H_2 molecules was predicted to be the optimal configuration for hydrogen adsorption. For this configuration at 10 MPa a maximum storage capacity of 1.3 wt % or $14\,kg/m^3$ was predicted.

In another report by Wang and Johnson the strength of the solid–fluid interaction was increased in an effort to identify a combination of potential and geometry that would allow for hydrogen-storage densities in SWNTs that would approach the DOE target values [65]. It was found that at ambient temperature the DOE target could not be reached even by tripling the fluid–wall potential. Only by doubling the interaction potential at 77 K was the DOE target able to be met. It was next attempted to study the adsorption of hydrogen by nanotubes with a charge of $\pm 0.1\,e^-/C$ [67]. An increase in adsorption relative to uncharged tubes of $\sim 10 - 20\%$ at 298 K and $15 - 30\%$ at 77 K was predicted. However, the charged nanotube arrays still did not enable the DOE target to be met at ambient temperature unless the charge on the nanotube was unrealistically large.

Two very recent theoretical studies have predicted adsorption capacities in relatively good agreement with the high-pressure H_2-adsorption investigations of Ye et al. [56] where a hydrogen adsorption at 8 wt % was observed at 77 K for purified laser-generated SWNTs. Employing Monte Carlo simulations to SWNTs which were arranged in a square lattice rather than a hexagonal lattice, a maximum hydrogen-adsorption capacity of 11.2 wt % was predicted for 2.2-nm diameter tubes at 77 K and 10 Mpa [71]. Another Monte Carlo simulation predicted a maximum excess gravimetric storage capacity of 9.6 wt % for an isolated 1.3-nm diameter tube at 77 K and 10 MPa. Under the same conditions, bundles containing 3 and 7 SWNTs were predicted to store 7.0- and 5.5-wt % hydrogen, respectively [70]. In a recent study which performed density functional calculations to predict both adsorption sites and maximum storage capacities, two possible chemisorption sites at the end of an open SWNT were predicted. The maximum storage capacity of molecular hydrogen inside the SWNTs was limited by both the repulsive energies between the H_2 molecules and between the H_2 molecules and the nanotube walls. The hydrogen-storage capacity of 1.3-nm diameter nanotubes was predicted to ex-

ceed 160-kg H_2/m^3 and 14 wt % [72]. In contrast, a different molecular modeling study employing density functional theory predicted that idealized adsorbent structures of single-walled carbon nanotubes would have adsorption capacities of only $\sim 1-2$ wt % at 60 MPa for temperatures between 150–315 K. However, the authors discussed possible mechanisms by which the gravimetric densities could be increased including chemisorption, adsorption at interstitial sites and swelling of the nanotube array [73].

3 Future: optimizing and understanding the interaction between hydrogen and carbon materials

From the above analysis it is apparent that if carbon adsorbents are to ultimately be applied in a hydrogen-storage system, many advances remain to be made. It is obviously important to maximize the hydrogen-adsorption capacity for a given carbon system at room temperature and for moderate pressures. It is equally important that the system both charges and discharges rapidly and completely at near ambient conditions. In order to optimize a carbon-based hydrogen-storage system it will be necessary to obtain a better understanding of the adsorption mechanism and to determine the precise adsorption sites in the carbon network that are responsible for the more promising adsorption properties. When optimization is complete, it will be necessary to scale up the synthetic and purification techniques that generate the ideal adsorption materials. The development of industrial-scale, cost-effective procedures will of course be mandatory.

To date the hydrogen-adsorption process that has been analyzed the most thoroughly is that which occurs on single-walled carbon nanotubes. Some of the more recent theoretical studies [70, 71] are in good agreement with the experimental data acquired for low-temperature, high-pressure adsorption on purified laser-generated SWNTs [56]. The fact that theoretical predictions do not account for the high H_2-adsorption capacities observed at room temperature for arc-generated SWNTs [45, 58] as well as for cut laser-generated SWNTs [59, 60] implies that elements of the adsorption mechanism which are active here are not yet well understood. It is likely that arc-generated tubes are synthesized with more defects and that the bundles are smaller and formed with a higher degree of disorder than the long crystalline ropes obtained by the method of laser vaporization [48]. The polydispersity of nanotube diameters within bundles may also be different for arc-material. Finally, it is probable that the SWNTs are functionalized, damaged and disordered during purification, cutting or pretreatments in acid. Most of the simulation studies thus far have used idealized models of nanotubes. Defect sites and disorder have not been considered, and the nanotubes forming a given bundle have always been mono-disperse. Molecular simulations which consider the effects of packing disorder, diameter polydispersity, functionalization and nanotube wall defects are currently under way [74]. Investigations such as these may enable a much better understanding of the aspects crucial to obtaining optimal storage capacities.

It is also necessary to understand the precise nature of the interaction between hydrogen and a given carbon surface. Is it a purely physical or chemical interaction or is it perhaps somewhere in between? A recent experimental report on electrochemical H_2 storage in MWNTs and SWNTs displayed a Raman feature at 4226 cm^{-1} for the charged materials, which was attributed to molecular hydrogen physisorbed on the nanotubes. However, the data is in doubt since no second-order Raman features were observed by the authors for the SWNTs [61]. A second-order feature at ~ 4260 cm^{-1} should be clearly observed even for relatively impure samples [75]. Since the SWNT Raman modes are resonantly enhanced [76] while the molecular hydrogen mode is not, it seems highly unlikely that the mode observed at 4226 cm^{-1} in this study may be attributed to hydrogen which is physisorbed on the SWNT carbon nanotubes. The Raman spectrum of the SWNT sample indicates that it is highly impure. The fact that no information is given on the purity of the MWNT samples makes a specific assignment of the feature at 4226 cm^{-1} in the MWNT spectrum quite difficult as well. Both infrared and Raman investigations on hydrogen-charged high-capacity purified samples of SWNTs are presently under way in an effort to better understand the nature of the carbon–hydrogen interaction [77]. Concurrently, theoretical investigations probing the nature of the SWNT–hydrogen interaction are being performed [78]. Nuclear magnetic resonance studies and inelastic neutron-scattering measurements on homogeneous carbon adsorbents which contain relatively high concentrations of hydrogen are also warranted.

Another crucial piece of knowledge which is necessary to optimize a given carbon-adsorbent system is the precise location of the adsorption sites. For example, is the adsorption site that may be depopulated at 300 K for cut and purified laser-generated SWNTs [59, 60] located on larger diameter tubes rather than smaller diameter tubes? This may perhaps be determined by conducting adsorption studies on materials which have been generated by the recently developed techniques for the controlled laser-generation of SWNTs with specific diameters [55, 79]. Is it also possible that either semiconducting or metallic SWNTs are better suited for hydrogen adsorption? Raman studies at multiple wavelengths which enable the differentiation between semiconducting and metallic nanotubes [80] may enable an answer to this question. If a preference is determined, synthetic methods for the production of specific metallic or semiconducting tubes will need to be developed.

After a hydrogen-adsorption material is optimized, it will then be necessary to focus on scaling up the production of the given adsorbent material. It is likely that this will be a fairly lofty task. For example, if the system is SWNT-based, current state-of-the-art production and purification techniques at best provide gram quantities of high-quality material per day. New chemical vapor deposition synthetic techniques for the growth of SWNTs are currently being developed [81–84], which may be more amenable to cost-effective industrial production processes. However, it has yet to be determined if SWNTs produced by CVD methods may be easily purified and whether they are suitable for hydrogen-adsorption applications. Ultimately, a better understanding of the unique interactions of hydrogen with carbon-adsorbent surfaces is required so that the optimal storage materials may be identified. These aspects will be the focus of research in the years to come.

Acknowledgements. This work was supported by the Office of Science, Basic Energy Sciences, Division of Materials Science and the Office of Energy Efficiency and Renewable Energy Hydrogen Program of the Department of Energy under Grant No. DE-AC36-99GO10337.

References

1. H.-H. Rogner: Int. J. Hydrogen Energy **23**(9), 833 (1998)
2. A.J. Kidnay, M.J. Hiza: Adv. Cryog. Eng. **12**, 730 (1967)
3. A.S. Coolidge: J. Am. Chem. Soc. **56**, 54 (1934)
4. S. Hynek, W. Fuller, J. Bentley, J. McCullough: In *Hydrogen Energy Progress X*, ed. by D.L. Block, T.N. Veziroglu (International Association for Hydrogen Energy, Coral Gables, FL 1994) pp. 985–1000
5. C. Carpetis, W. Peschka: Int. J. Hydrogen Energy **5**, 539 (1980)
6. C. Carpetis, W. Peschka: *On the storage of hydrogen by use of cryoadsorbents*, In Proc. 1st World Hydrogen Energy Conference (1976) paper 9C-45
7. R.K. Agarwal, J.S. Noh, J.A. Schwarz, P. Davini: Carbon **25**, 219 (1987)
8. J.S. Noh, R.K. Agarwal, J.S. Schwarz: Int. J. Hydrogen Energy **12**, 693 (1987)
9. J.A. Schwarz: Final Report for the Tasks XC-1-1108-1 and XAE-3-13346-01 (National Renewable Energy Laboratory, Golden Colorado 1994)
10. J.A. Schwarz: In *Proc. 1993 DOE/NREL Hydrogen Program Review* (1993) pp. 89–102
11. R. Chahine, P. Bénard: *Performance study of hydrogen adsorption storage systems, In Hydrogen Energy Progress XII*, ed. by J.C. Bolcich, T.N. Veziroglu (International Association of Hydrogen Energy, Coral Gables, 1998) pp. 979–986
12. S. Hynek, W. Fuller, J. Bentley: Int. J. Hydrogen Energy **22**(6), 601 (1997)
13. R. Chahine, T.K. Bose: Int. J. Hydrogen Energy **19**, 161 (1994)
14. S. Orimo, G. Majer, T. Fukunaga, A. Zuttel, L. Schlapbach, H. Fujii: Appl. Phys. Lett. **75**(20), 3093 (1999)
15. D.F. Quinn, J.A. MacDonald: Carbon **30**, 1097 (1992)
16. N.M. Rodriguez, A. Chambers, R.T.K. Baker: Langmuir **11**, 3862 (1995)
17. A. Chambers, C. Park, R.T.K. Baker, N.M. Rodriguez: J. Phys. Chem. B **102**, 4253 (1998)
18. M. Nielsen, J.P. McTague, W. Ellenson: J. Phys. **38**, C4 (1977)
19. C.C. Ahn, Y. Ye, B.V. Ratnakumar, C. Whitham, R.C. Bowman, B. Fultz: Appl. Phys. Lett. **73**, 3378 (1998)
20. R. Strobel, L. Jorissen, T. Schlier, V. Trapp, W. Schulz, K. Bohmhammel, G. Wolf, J. Garche: J. Power Sci. **84**, 221 (1999)
21. C. Park, P.E. Anderson, A. Chambers, C.D. Tan, R. Hidalgo, N.M. Roderiguez: J. Phys. Chem. B. **103**, 10572 (1999)
22. Y.-Y. Fan, B. Liao, M. Liu, Y.-L. Wei, M.-Q. Lu, H.-M. Cheng: Carbon **37**, 1649 (1999)
23. X.K. Wang, X.W. Lin, V.P. Dravid, J.B. Ketterson, R.P.H. Chang: Appl. Phys. Lett. **66**, 427 (1995)
24. G.L. Dell, P.C. Eklund, G. Senatore: *Intercalation in Layered Materials*, ed. by M.S. Dresselhaus (Plenum Press, New York 1986)
25. N. Hatta, K. Murata: Chem. Phys. Lett. **217**, 398 (1994)
26. S. Iijima: Nature **354**, 56 (1991)
27. T.W. Ebbesen, P.M. Ajayan: Nature **358**, 220 (1992)
28. M. Ishigami, J. Cumings, A. Zettl, S. Chen: Chem. Phys. Lett. **319**, 457 (2000)
29. M. Endo, K. Takeuchi, S. Igarashi, K. Kobori, M. Shiraishi, H.W. Kroto: J. Phys. Chem. Solids **54**, 1841 (1993)
30. M. Jose-Yacaman, M. Miki-Yoshida, L. Rendon, J.G. Santiesteban: Appl. Phys. Lett. **62**, 202 (1993)
31. V. Ivanov, J.B. Nagy, P. Lambin, A. Lucas, X.B. Zhang: Chem. Phys. Lett. **223**, 329 (1994)
32. J.-F. Colomer, P. Piedigrosso, I. Wilems, C. Journet, P. Bernier, G. Van Tendeloo, A. Fonseca, J.B. Nagy: J. Chem. Soc. Faraday Trans. **94**, 3753 (1998)
33. T.W. Ebbesen, P.M. Ajayan, H. Hiura, K. Tanigaki: Nature **367**, 519 (1994)
34. G.L. Hornyak, A.C. Dillon, P.A. Parilla, J.J. Schneider, N. Czap, K.M. Jones, F.S. Hasoon, A. Mason, M.J. Heben: Nanostruct. Mater. **12**, 83 (1999)
35. P. Chen, X. Wu, J. Lin, K.L. Tan: Science **285**, 91 (1999)
36. M.S. Dresselhaus, K.A. Williams, P.C. Eklund: Mater. Res. Soc. Bull. **24**, 45 (1999)
37. R.T. Yang: Carbon **38**, 623 (2000)
38. F.E. Pinkerton, B.G. Wicke, C.H. Olk, G.G. Tibbetts, G.P. Meisner, M.S. Meyer, J.F. Herbst: J. Phys. Chem. B **104**(40), 9460 (2000)
39. X.B. Wu, P. Chen, J. Lin, K.L. Tan: Int. J. Hydrogen Energy **25**, 261 (2000)
40. C. Nutzenadel, A. Zuttel, D. Chartouni, L. Schlapbach: Electrochem. Solid-State Lett. **2**, 30 (1999)
41. S.J. Gregg, K.S.W. Sing: *Adsorption, Surface Area and Porosity* (Academic, London 1982)
42. S. Iijima, T. Ichihashi: Nature **363**, 603 (1993)
43. D.S. Bethune, C.-H. Kiang, M.S. de Vries, G. Gorman, R. Savoy, J. Vasquez, R. Beyers: Nature **363**, 605 (1993)
44. M.R. Pederson, J.Q. Broughton: Phys. Rev. Lett. **69**, 2689 (1992)
45. A.C. Dillon, K.M. Jones, T.A. Bekkedahl, C.H. Kiang, D.S. Bethune, M.J. Heben: Nature **386**, 377 (1997)
46. E.L. Pace, A.R. Siebert: J. Phys. Chem. **63**, 1398 (1959)
47. T. Guo, P. Nikolaev, A. Thess, D.T. Colbert, R.E. Smalley: Chem. Phys. Lett. **243**, 49 (1995)
48. A. Thess, R. Lee, P. Nikolaev, H. Dai, P. Pitit, J. Robert, C. Xu, Y.H. Lee, S.G. Kim, A.G. Rinzler, D.T. Colbert, G.E. Scuseria, D. Tomanek, J.E. Fischer, R.E. Smalley: **273**, 483 (1996)
49. K. Tohji, T. Goto, H. Takahashi, Y. Shinoda, N. Shimizu, B. Jeyadevan, I. Matsuoka, Y. Saito, A. Kasuya, T. Ohsuna, K. Hiraga, Y. Nisshina: Nature **383**, 679 (1996)
50. S. Bandow, A.M. Rao, K.A. Williams, A. Thess, R.E. Smalley, P.C. Eklund: J. Phys. Chem. B **101**, 8839 (1997)
51. E. Dujardin, T.W. Ebbesen, A. Krishnan, M.M.J. Treacy: Adv. Mater. **10**, 611 (1998)
52. K.B. Shelimov, R.O. Esenaliev, A.G. Rinzler, C.B. Huffman, R.E. Smalley: Chem. Phys. Lett. **282**, 429 (1998)
53. A.G. Rinzler, J. Lui, H. Dai, P. Nikolaev, C.B. Huffman, F.J. Rodericguez-Macias, P.J. Boul, A.H. Lu, D. Heymann, D.T. Colbert, R.S. Lee, J.E. Fischer, A.M. Rao, P.C. Eklund, R.E. Smalley: Appl. Phys. A **67**, 29 (1998)
54. A.C. Dillon, T. Gennett, K.M. Jones, J.L. Alleman, P.A. Parilla, M.J. Heben: Adv. Mater. **11**, 1354 (1999)
55. A.C. Dillon, P.A. Parilla, J.L. Alleman, J.D. Perkins, M.J. Heben: Chem. Phys. Lett. **316**, 13 (2000)
56. Y. Ye, C.C. Ahn, C. Witham, B. Fultz, J. Liu, A.G. Rinzler, D. Colbert, K.A. Smith, R.E. Smalley: Appl. Phys. Lett. **74**, 2307 (1999)
57. C.M. Brown, T. Yildirim, D.A. Neuman, M.J. Heben, T. Gennett, A.C. Dillon, J.L. Alleman, J.E. Fischer: Chem. Phys. Lett. **329**, 311 (2000)
58. C. Liu, Y.Y. Fan, M. Liu, H.T. Cong, H.M. Cheng, M.S. Dresselhaus: Science **286**, 1127 (1999)
59. A.C. Dillon, T. Gennett, J.L. Alleman, P.A. Parilla, K.M. Jones, G.L. Hornyak: Proc. Mat. Res. Soc. in press
60. A.C. Dillon, T. Gennett, J.L. Alleman, K.M. Jones, P.A. Parilla, M.J. Heben: In *Proc. 2000 U.S. D.O.E. Hydrogen Program Review* (2000)
61. S.M. Lee, K.S. Park, Y.C. Choi, Y.S. Park, J.M. Bok, D.J. Bae, K.S. Nahm, Y.G. Choi, S.C. Yu, N.G. Kim, T. Frauenheim, Y.H. Lee: Synth. Met. 113, 209 (2000)
62. M.S. Dresselhaus, K.A. Williams, P.C. Eklund: Mater. Res. Soc. Bull. **24**, 45 (1999)
63. G. Stan, M.W. Cole: J. Low Temp. Phys. **110**, 539 (1998)
64. F. Darkrim, P. Malbrunot, D. Levesque: In *Hydrogen Energy Progress XII*, ed. by J.C. Bolcich, T.N. Veziroglu (International Association for Hydrogen Energy, Corel Gables, FL 1998) pp. 985–1000
65. Q. Wang, J.K. Johnson: J. Phys. Chem. B **103**, 4809 (1999)
66. Q. Wang, J.K. Johnson: J. Chem. Phys. B **110**, 577 (1999)
67. V.V. Simonyan, P. Diep, J.K. Johnson: J. Chem. Phys. **111**, 9778 (1999)
68. M. Rzepka, P. Lamp, M.A. de la Casa-Lillo: J. Phys. Chem. **102**, 10894 (1998)
69. F. Darkrim, D. Levesque: J. Chem. Phys. **109**, 4981 (1998)
70. K.A. Williams, P.C. Eklund: Chem. Phys. Lett. **320**, 352 (2000)
71. F. Darkrim, D. Levesque: J. Phys. Chem. B **104**, 6773 (2000)
72. S.M. Lee, Y.H. Lee: Appl. Phys. Lett. **76**, 2877 (2000)
73. P.A. Gordon, R.B. Saeger: Ind. Eng. Chem. Res. **38**, 4647 (1999)
74. V.V. Simonyan, J.K. Johnson: in preparation
75. P. Tan, Y. Tang, Y.M. Deng, F. Li, Y.L. Wei, H.M. Cheng: Appl. Phys. Lett. **75**, 1524 (1999)

76. A.M. Rao, E. Richter, S. Bandow, B. Chase, P.C. Eklund, K.A. Williams, S. Fang, K.R. Subbaswamy, M. Menon, A. Thess, R.E. Smalley, G. Dresselhaus, M.S. Dresselhaus: Science **275**, 187 (1997)
77. A.C. Dillon, T. Gennett, L. Grigorian, P.A. Parilla, J.L. Alleman, D.L. Young, K.M. Jones, G.L. Hornyak, M.J. Heben: in preparation
78. H. Cheng, G. Pez, A. Cooper: in preparation
79. S. Bandow, S. Asaka, Y. Saito, A.M. Rao, L. Grigorian, E. Richter, P.C. Eklund: Phys. Rev. Lett. **80**, 3779 (1998)
80. S.D.M. Brown, P. Corio, A. Marucci, M.S. Dresselhaus, M.A. Pimenta, K. Kneipp: Phys. Rev. B **61**, R5137 (2000)
81. J.H. Hafner, M.J. Bronikowski, B.R. Azamian, P. Nikolev, A.G. Rinzler, D.T. Colbert, K.A. Smith, R.E. Smalley: Chem. Phys. Lett. **296**, 195 (1998)
82. H.M. Cheng, F. Li, G. Su, H.Y. Pan, L.L. He, X. Sun, M.S. Dresselhaus: Appl. Phys. Lett. **72**, 3282 (1998)
83. A.M. Cassell, A. Raymakers, J. Kong, H. Dai: J. Phys. Chem. B **103**, 6484 (1999)
84. J.-F. Colomer, C. Stephan, S. Lefrant, G. Van Tendeloo, I. Willems, Z. Koyna, A. Fonesca, C. Laurent, J.B. Nagy: Chem. Phys. Lett. **317**, 83 (2000)